Published in Physical Review Letters 96, issue 7, 1150-1153, 1996
which should be used for any reference to this work

k-Space Mapping of Majority and Minority Bands on the Fermi Surface of Nickel below and above the Curie Temperature

P. Aebi,[1] T. J. Kreutz,[2] J. Osterwalder,[2] R. Fasel,[1] P. Schwaller,[2] and L. Schlapbach[1]
[1]*Institut de Physique, Université de Fribourg, CH-1700 Fribourg, Switzerland*
[2]*Physik Institut, Universität Zürich-Irchel, CH-8057 Zürich, Switzerland*

A section through the three-dimensional Fermi surface of Ni has been mapped perpendicular to the [110] direction using angle-scanned photoemission. Regions of minority and majority spin bands, well separated in *k* space, can clearly be identified through comparison with a band structure calculation. The behavior of the different bands is observed for temperatures below and above the Curie temperature T_C. We find bands which move and bands which stay in place for going from $T < T_C$ to $T > T_C$.

Despite a large amount of experimental data on the electronic and magnetic structure of nickel, conflicting conclusions persist about the behavior of the exchange splitting ΔE_{ex} as a function of temperature [1–5]: While some experiments point to a largely temperature-independent exchange splitting in going across the Curie temperature ($T_C = 631$ K) others give evidence for changes of the Fermi surface (FS) in traversing T_C. Insight into this question has also been gained from photoemission and inverse photoemission experiments [6–12], and again conflicting views were obtained with respect to the temperature dependence of ΔE_{ex}. Recent experiments found that spin-split bands merged with temperature at some $\mathbf{k}$ locations while their splitting remained temperature independent at others [10]. Inverse photoemission studies [12] reported on collapsing spin-split bands upon approaching T_C even for the magnetic Z_2 band, and the experimentally determined exchange splitting followed the rescaled bulk magnetization curve.

Considering these results showing both temperature-independent or collapsing exchange splittings, and thus indicating at the same time the persistence of local moments and a Stoner-type behavior, it is important to obtain a more systematic view of the temperature behavior of ΔE_{ex} in $\mathbf{k}$ space, and, in particular, of the magnetic bands crossing the Fermi level (E_F). We therefore present a high-resolution temperature-dependent mapping of a complete section through the FS of Ni, as viewed through the (110) surface, in which several magnetic bands are observed at the same time. It is important to note that the present experiment resolves majority and minority bands in $\mathbf{k}$ space.

Recently, Santoni *et al.* [13] used a two-dimensional display-type analyzer to map the FS of layered graphite directly by measuring the total photoelectron intensity within a narrow energy window at E_F. High intensities are recorded at locations of the wave vector component parallel to the surface ($\mathbf{k}_{\parallel}$) where direct transitions disperse through this window, namely, through the FS. In the present work we use sequential angle-scanning data acquisition [14], providing a high energy resolution and access to a wide range in $\mathbf{k}$ space. Recently we demonstrated the efficiency and accuracy of this method by measuring the two-dimensional FS of a Bi cuprate [15] and cuts through the three-dimensional FS of Cu [16]. The obvious advantage of this procedure is that it provides a very accurate intensity mapping with a selectable uniform sampling density. In contrast to conventional photoemission experiments measuring complete energy-distribution curves (EDC's), but at fewer locations in the Brillouin zone (BZ), the present measurement will not miss any direct transitions crossing E_F. The experimental procedure was outlined in Refs. [14–16], and we refer the reader to this work for details.

In Fig. 1(a) we present the room temperature (RT) $\mathbf{k}_{\parallel}$ mapping of the intensity of He I excited photoelectrons collected within an energy window of about 30 meV, determined by the instrumental energy resolution, centered at E_F. The outer circle corresponds to a polar angle of 90°, and the center of the image represents normal emission. Intensities are linearly color coded as indicated in the color bar. High intensities result at $\mathbf{k}_{\parallel}$ locations where direct transitions move through E_F, yielding therefore a FS of Ni. These locations show up as relatively fine, well defined lines. Judging from these data, the violation of the conservation of the wave vector component perpendicular to the surface ($\mathbf{k}_{\perp}$) does not appear to be too severe. The mapping corresponds to a section through the FS perpendicular to the [110] direction as has been demonstrated in [16] for the example of Cu. Intensities are modulated along these lines due to matrix element effects.

We distinguish several sets of lines, which we label A, B, and C in Fig. 1(a), as well as their symmetry-related counterparts. Since our experiment is not inherently spin resolved, we have to compare these data to the result of a spin-polarized FS calculation in order to determine which lines correspond to the majority FS (which should be essentially *sp*-like as the majority *d* band is filled) and which to the minority FS. In Fig. 1(c) we display the result of a calculation using the spin-polarized layer Korringa-Kohn-Rostoker (LKKR) formalism [17],

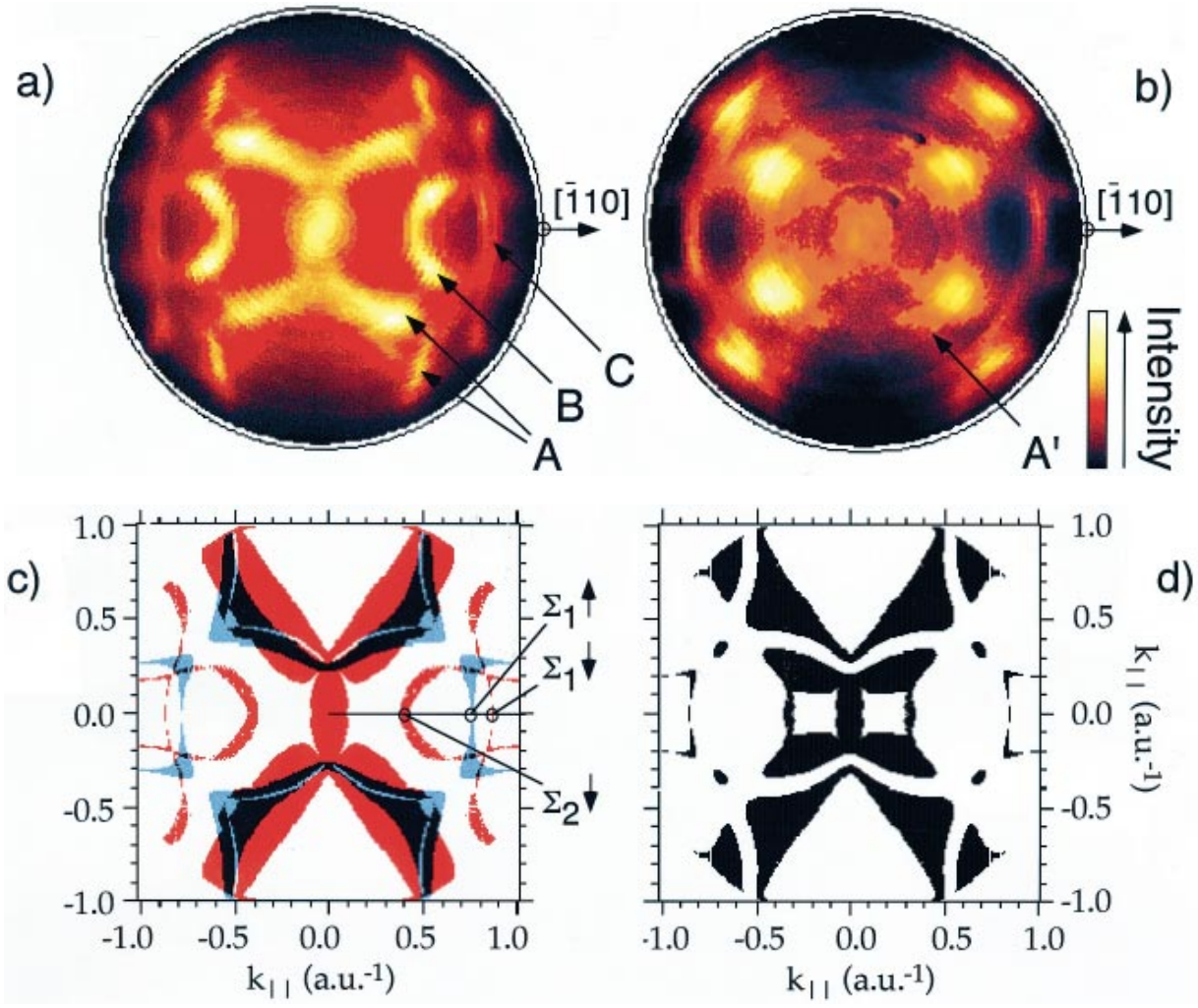

FIG. 1(color). (a) RT ($T/T_C \sim 0.48$) mapping of the intensity of He I (21.2 eV) excited photoelectrons collected within an energy window of about 30 meV centered at E_F, linear in $\mathbf{k}_\parallel$. The outer circle indicates an emission angle of 90°, the center represents normal emission or $\mathbf{k}_\parallel = 0$. Intensities are given in a linear color code as indicated in the color bar. (b) Same as (a) but for $T/T_C \sim 1.1$. (c) Calculated cut through the bulk FS using the spin-polarized LKKR scheme for the initial state and a free-electron final state (see text). Majority spins are given in blue and minority spins in red. (d) LKKR calculation as in (c) but unpolarized.

stacking (111) layers up to convergence. Calculations along high symmetry directions agree well with published band calculations such as [18]. For a given energy and $\mathbf{k}_\parallel$, this code delivers the corresponding eigenvalues $\mathbf{k}_\perp$ of the Bloch functions for majority and minority spins and hence their constant energy surface. Assuming a one-beam free electron approximation for the photoelectron final state in the extended BZ as described in Ref. [16] a spherical section through the calculated FS is created. An inner potential of 10.7 eV [19] and a work function of 4.7 eV were assumed. In order to allow a point to be plotted in the calculation of Fig. 1(c) a maximum difference of 0.1 inverse atomic units (a.u.$^{-1}$) between the free electron $\mathbf{k}_\perp$ and the calculated $\mathbf{k}_\perp$ on the FS is accepted. No attempt has been made to optimize parameters in the calculation. We find that while majority (blue) and minority (red) spin bands overlap in some regions they are well separated in others. Consulting a recent band structure calculation along high-symmetry directions by Eckardt and Fritsche [20] we can identify the three locations marked in Fig. 1(c) with the Fermi-level crossings of the minority *d* band near the Σ line (named $\Sigma_2^\downarrow$) and of the spin-split *sp* bands between the Δ and the Σ lines (named $\Sigma_1^\uparrow$ and $\Sigma_1^\downarrow$) [21].

Comparing Figs. 1(c) and 1(a) we find an excellent agreement of intensity lines in the data with the calculated FS section. Indeed, the agreement is of a quality that it is justified to use this calculation in order to spin label the observed lines in the experiment. In this way the majority and minority bands can be well separated just by their different locations in *k* space. Moreover, this agreement indicates that our experiment is representative for the bulk magnetism, since surface effects are not included in the calculations. The feature B can be identified with the magnetic minority *d* band, including $\Sigma_2^\downarrow$. The splitting of the *sp* band ($\Sigma_1^\uparrow$ and $\Sigma_1^\downarrow$) is also well resolved in the

experiment, which is more obvious in Fig. 2(a), providing a polar section through the data of Fig. 1(a) along the $[\bar{1}10]$ azimuth.

At this point we have to briefly comment upon the relation of the data in Fig. 1(a) to a conventional FS measurement. The photoemission experiment with $h\nu = 21.2$ eV "takes place" in the second BZ. Therefore, as indicated in Fig. 3 [22], the $\mathbf{k}_{\parallel}$ measured in tilting the electron detection angle away from the normal is along X'-Γ_{020} (and not Γ_{000}-K) if one tilts towards $[\bar{1}10]$. This explains the fact that in Fig. 1(a) one observes with increasing $\mathbf{k}_{\parallel}$ along the $[\bar{1}10]$ direction the ordering $\Sigma_2^{\downarrow}$, $\Sigma_1^{\uparrow}$, and $\Sigma_1^{\downarrow}$, which is reversed from that in the first BZ. To make the connection with the ordinary Brillouin zone obvious we give in Fig. 4 one quadrant of the BZ in the (001) plane containing the results of a de Haas–van Alphen (dHvA) experiment (open symbols [23]) and data obtained from Fig. 1(a) (filled ellipses). The dashed line follows the locations scanned during the polar scan, as indicated in Fig. 3. The E_F crossings [Fig. 1(a) and 2(a)] are represented by ellipses with dimensions reflecting approximately the experimental widths of the transitions. We find three intensity maxima in good coincidence with crossings of the FS observed by dHvA measurements.

Figure 1(b) shows a FS map analogous to that of Fig. 1(a) but for a temperature corresponding to a value of $T/T_C \sim 1.1$. Noticeable changes occur. The changes between Figs. 1(a) and 1(b) occur smoothly with temperature [24]. We find regions where lines are considerably broader than in Fig. 1(a), while others remain as fine as before. Measurements performed on Cu for comparison under the same conditions stay virtually unchanged [24]. Therefore we are assured to observe the influence of temperature on the magnetism of Ni over an extended region in k space.

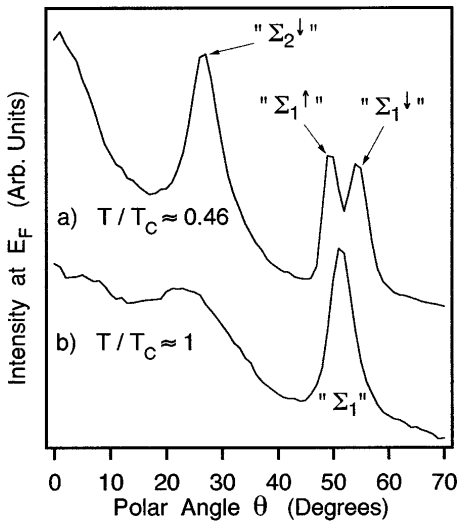

FIG. 2. (a) Polar section through the RT intensity map of Fig. 1(a) along the $[\bar{1}10]$ azimuth. (b) Same as in (a) but for $T/T_C \sim 1$.

A very obvious change happens to the feature C in Fig. 1(a), which is related to the *sp* band ($\Sigma_1^{\uparrow}$ and $\Sigma_1^{\downarrow}$): The splitting collapses but the line remains rather fine. This is clearly seen in the section given in Fig. 2(b) indicating also that phonon effects as described in [25] for x-ray excitation do not seem to play an important role here. In this same figure one finds a different behavior for the *d* band related feature B ($\Sigma_2^{\downarrow}$), which becomes much broader and shows, if at all, a slight shift towards lower polar angles. The overall amount of diffuse intensity also increases with temperature. This seems to be related with the magnetism or at least with the flat bands of Ni since the measurements on Cu do not show such a behavior [24]. Furthermore we observe a change of the feature in the center of Fig. 1(a), which does not disappear upon heating, but changes its relative weight in Fig. 1(b).

It is not obvious from the calculation in Fig. 1(c) to assess which is the spin character of bands that move in the region of feature A since minority bands, with mainly *d* character at E_F and majority bands with mainly *sp* character at E_F are degenerate. But we can say that some bands (A, B) move while others do not (A′). This is not consistent with a simple Stoner picture where all bands are expected to move smoothly. Also, the increase of diffuse intensity indicates a more complex behavior. This is further confirmed by the calculation given in Fig. 1(d), which represents the FS obtained by the unpolarized LKKR method. Clearly, the agreement with the high-temperature experiment [Fig. 1(b)] is poor except for the

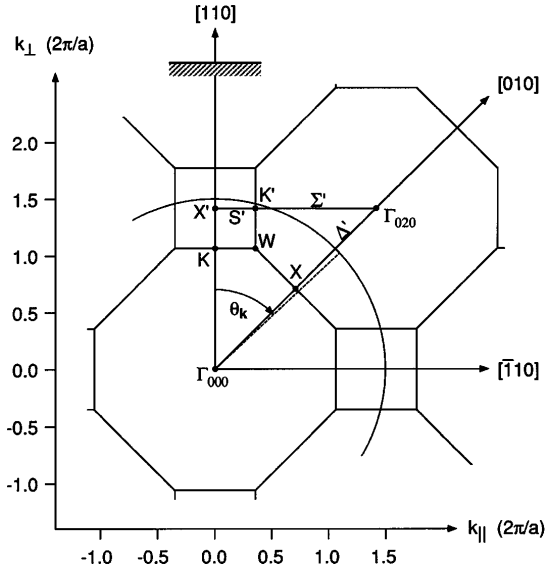

FIG. 3. View of the (001) plane in reciprocal space, indicating the Brillouin zone boundaries for Ni in the extended zone scheme [22]. High-symmetry points and lines are indicated as well as the [110] surface normal. The circle represents the free-electron final-state wave vectors for emission from the Fermi edge at a photon energy of 21.2 eV. The full range of polar emission angles θ is indicated by the curved arrow.

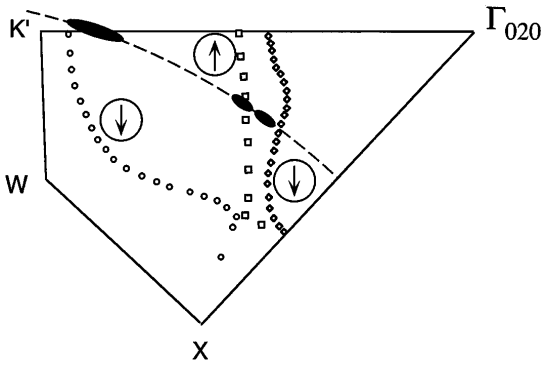

FIG. 4. Fermi surface cross sections of Ni in the (001) plane obtained from de Haas–van Alphen experiments (open symbols, from Ref. [23]) compared to the data extracted from Fig. 1(a) (filled ellipses).

sp-like feature C, where the collapse of the splitting as well as the position is quite well reproduced.

Movements of bands on the FS must also be associated with changes in band filling. We have probed the dispersion of the bands near the FS at RT by taking similar constant energy surfaces for energies slightly above and below E_F in order to address this question (not shown [24]). In fact, we find a similar coalescence of features A and B for an intensity map at $E_F + 100$ meV, which is far in the tail of the Fermi function. One possible interpretation of our high-temperature data is thus that we have moved upward the chemical potential in the minority band by roughly 100 meV, which is about half way of typical values for ΔE_{ex}. Naturally, this rigid-band-like shift should be compensated by an opposite shift of majority bands in order to maintain a constant electron number. Again, in a constant energy scan at $E_F - 150$ meV we find a similar pileup of intensity in the region between features A and B. Together with the observed collapse of the splitting in the *sp* band (feature C), these phenomena indicate a Stoner-like behavior.

In summary, we have presented a high-resolution photoemission measurement of a complete section through the FS of Ni providing macroscopically averaged *local* information on the electronic and magnetic structure and agreeing with conventional data. We find that majority and minority bands can be separated by their different locations in *k* space. The measurement for $T > T_C$ shows both bands moving and joining each other and bands remaining in place. These experiments provide a systematic view on which bands follow a Stoner-type picture and which show a more complex behavior. A measurement of the temperature dependence of the shape of the FS of Ni is difficult with conventional techniques, while it is obviously easy with the technique presented here.

We are indebted to S. Hüfner for stimulating discussions and for critically reading the manuscript. Skillful technical assistance was provided by F. Bourqui, E. Mooser, O. Raetzo, and H. Tschopp. This project has been supported by the Fonds National Suisse pour la Recherche Scientifique.

[1] For a review, see H. Capellmann, J. Magn. Mater. **28**, 250 (1982).
[2] J. Kirschner and E. Langenbach, Solid State Commun. **66**, 761 (1988).
[3] P. Genoud, A. A. Manuel, E. Walker, and M. Peter, J. Phys. Condens. Matter **3**, 4201 (1991).
[4] G. Shirane, O. Steinsvoll, Y. J. Uemura, and J. Wicksted, J. Appl. Phys. **55**, 1887 (1984).
[5] M. Yousuf, P. Ch. Sahu, and K. G. Rajan, Philos. Mag. B **54**, 241 (1986).
[6] M. Donath, Surf. Sci. Rep. **20**, 251 (1994).
[7] D. E. Eastman, F. J. Himpsel, and J. A. Knapp, Phys. Rev. Lett. **40**, 1514 (1978).
[8] C. J. Maetz, U. Gerhardt, E. Dietz, A. Ziegler, and R. J. Jelitto, Phys. Rev. Lett. **48**, 1686 (1982).
[9] H. Hopster, R. Raue, G. Güntherodt, E. Kisker, R. Clauberg, and M. Campagna, Phys. Rev. Lett. **51**, 829 (1983).
[10] K.-P. Kämper, W. Schmitt, and G. Güntherodt, Phys. Rev. B **42**, 10 696 (1990).
[11] A. Kakizaki, J. Fujii, K. Shimada, A. Kamata, K. Ono, K.-H. Park, T. Kinoshita, T. Ishii, and H. Fukutani, Phys. Rev. Lett. **72**, 2781 (1994).
[12] W. von der Linden, M. Donath, and V. Dose, Phys. Rev. Lett. **71**, 899 (1993).
[13] A. Santoni, L. J. Terminello, F. J. Himpsel, and T. Takahashi, Appl. Phys. A **52**, 229 (1991).
[14] J. Osterwalder, T. Greber, A. Stuck, and L. Schlapbach, Phys. Rev. B **44**, 13 764 (1991); D. Naumović, A. Stuck, T. Greber, J. Osterwalder, and L. Schlapbach, Phys. Rev. B **47**, 7462 (1993).
[15] P. Aebi, J. Osterwalder, P. Schwaller, L. Schlapbach, M. Shimoda, T. Mochiku, and K, Kadowaki, Phys. Rev. Lett. **72**, 2757 (1994).
[16] P. Aebi, J. Osterwalder, R. Fasel, D. Naumović, and L. Schlapbach, Surf. Sci. **307–309**, 917 (1994).
[17] J. M. MacLaren, S. Crampin, D. D. Vvedensky, R. C. Albers, and J. B. Pendry, Comput. Phys. Commun. **60**, 365 (1990).
[18] V. L. Moruzzi, J. F. Janak, and A. R. Williams, *Calculated Electronic Properties of Metals* (Pergamon, New York, 1978).
[19] W. Eberhardt and E. W. Plummer, Phys. Rev. B **21**, 3245 (1980).
[20] H. Eckardt and L. Fritsche, J. Phys. F **17**, 925 (1987).
[21] T. J. Kreutz, P. Aebi, and J. Osterwalder, Solid State Commun. **96**, 339 (1995).
[22] A Fermi surface cross section obtained from calculation and de Haas–van Alphen experiments plotted within the K′WXΓ wedge can be found in Fig. 6 of Ref. [20].
[23] Unpublished results of Stark; see C. S. Wang and J. Callaway, Phys. Rev. B **9**, 4897 (1974).
[24] T. Kreutz, P. Aebi, J. Osterwalder, and L. Schlapbach, J. Electron Spectrosc. Relat. Phenom. (to be published).
[25] Z. Hussain, C. S. Fadley, S. Kono, and L. F. Wagner, Phys. Rev. B **22**, 3750 (1980).